ENGINEERING RESEARCH INSTITUTE
THE UNIVERSITY OF MICHIGAN
ANN ARBOR

Final Report

ON THE STRUCTURE OF JETS FROM HIGHLY UNDEREXPANDED NOZZLES INTO STILL AIR

T. C. Adamson, Jr.
J. A. Nicholls

ERI Project 2397

DEPARTMENT OF THE ARMY
DETROIT ORDNANCE DISTRICT
CONTRACT NO. DA-20-018-ORD-13821
DETROIT, MICHIGAN

February 1958

TABLE OF CONTENTS

SUMMARY

A method for calculating the position of the first normal shock, or Mach disc, in the jet behind a highly underexpanded nozzle is presented. In the calculation for a sonic orifice, the axial pressure distribution on the centerline of the flow behind the orifice, calculated by the method of characteristics, is used to define a fictitious nozzle extension, and the shock is then assumed to exist at that point where atmospheric pressure would be attained behind the shock, i.e., the shock is assumed to exist at the end of the fictitious nozzle extension. Physical arguments are then employed to extend this calculation to nozzles with supersonic exit Mach numbers. The results compare favorably with experimental data.

An approximate method for computing the jet boundary up to the point of maximum jet area is given, and the results are compared both with photographs of actual jets and with jet boundaries calculated by the method of characteristics. Favorable agreement exists at relatively low nozzle pressure ratios.

SYMBOLS

A = area

d = diameter of jet

M = Mach number

P = pressure

p = dimensionless static to total pressure ratio, P/P_t

r = radius of jet

x = axial coordinate

α = total divergence angle of jet boundary at nozzle exit

δ = divergence half angle of nozzle

ξ = dimensionless axial coordinate, x/d_N

ψ = angle made by jet boundary with axis of flow

θ = total angle between the tangent to the jet boundary at any point and the original jet flow direction, $\nu-\nu_e$

μ = Mach angle, $\sin^{-1}(1/M)$

ν = Prandtl-Meyer turning angle

γ = ratio of specific heats

Subscripts

t = total or stagnation conditions

∞ = conditions in atmosphere into which nozzle is exhausting

N = nozzle exit conditions

e = conditions at jet boundary immediately after expansion to atmospheric pressure.

m = conditions at Mach disc location

INTRODUCTION

The increased use of jet and rocket engines and recoilless rifles has caused a great deal of attention to be focused on the jet flow behind sonic and supersonic nozzles. In particular, the flow behind highly underexpanded nozzles is of great interest. A recent research program conducted by Love and Grigsby at the NACA Langley Aeronautical Laboratory,[1] for example, includes comprehensive experimental and theoretical studies of the structure of the jet flow behind nozzles of various configurations.

Fig. 1 is a sketch of the repeating flow picture generally observed behind an underexpanded axisymmetric nozzle. As the gas emerges from the exit, it goes through an expansion fan, expanding to the ambient pressure at the jet boundary, and then the condition of constant pressure along the jet boundary causes this boundary to be bent back toward the axis of flow. As the flow changes direction along this boundary, many compression waves, formed at the intersection of expansion waves with the jet boundary, are sent back into the flow; these waves coalesce to form the intercepting shock indicated in the sketch. For slightly underexpanded nozzles, these intercepting shocks meet at the axis, forming the familiar diamond configuration. As the pressure ratio across the nozzle is increased, however, these intercepting shocks no longer meet at the axis, but are connected with a normal shock, or Mach disc, as pictured in Fig. 1. In both cases, reflected shocks are formed, which intersect with the jet boundary, reflecting as expansion waves, and the whole process is repeated. The repetition is continued until viscous effects become predominant and this structure is no longer observed.

The study of the underexpanded jet, then, involves calculations of the jet boundary, the intercepting shock, the position of the first normal shock, and

the wavelength of the repeating structure. Experiment has indicated that, for a jet exhausting into a static atmosphere, the important parameters are the pressure ratio across the nozzle, the Mach number at the nozzle exit, and to a very slight degree, the divergence angle of the nozzle. The pressure ratio, in particular, has been used in several empirical relations for the wavelength and the distance between the nozzle exit and the Mach disc.[2,3] In this paper, only the downstream distances to the normal shock and the jet boundary are discussed. Furthermore, simple approximate methods of analysis are presented which allow these calculations to be made quite rapidly.

_.CATION OF THE FIRST MACH DISC

The downstream location of the first normal shock, or Mach disc, depends essentially on the pressure ratio across the nozzle and the exit Mach number, changing only slightly with the divergence angle of the nozzle for total divergence angles as high as 40°.[4,5] This indicates that the viscous effects must be rather insignificant for this calculation; otherwise, the angle at which the flow enters the atmosphere would be an important parameter, since the overall mixing area up to any downstream location increases with the initial boundary angle. Assuming viscous effects to be negligible, then, and noting that the main effects are due to the dynamic parameters, with no geometric complications, one is led to the conclusion that a simple quasi-one-dimensional calculation should give accurate results. In this event the problem is similar to the calculation of the shock position in a given nozzle, where isentropic, quasi-one-dimensional flow is assumed up to and beyond the shock. This idea is also strengthened by a consideration of the picture usually observed when a shock is located within a nozzle. The normal shock does not extend from surface to surface, but extends only to an intersection where a lambda configuration results; also, the flow separates from the wall slightly. However, in

spite of this fact, the location of the shock is fairly well predicted by disregarding the lambda configuration, and assuming the shock to be simply normal, extending across the whole fluid. Since the shock configuration occurring in the underexpanded jet is similar, although stretched out, it seems logical that there is a possibility of predicting the location of the normal shock without the necessity of calculating the whole shock structure. For the above reasons, then, the free jet was assumed to be simply an extension of the actual nozzle, bounded by a fictitious surface with an area distribution corresponding to the actual pressure distribution of the center, or core flow, up to the normal shock. The fictitious boundary extends only to the axial position of the shock wave, so as the total-to-atmospheric-pressure ratio changes, the length of the extension changes. Finally, since the pressure to which this fictitious nozzle is exhausting is atmospheric, the axial position of the shock is that point at which a shock has sufficient strength to bring the static pressure to atmospheric. In summary, the flow is assumed to be that through a nozzle with a shock at the exit. It is assumed to exhaust to atmospheric pressure at the exit. The nozzle configuration is that which corresponds to a given axial pressure distribution in the center or core of the actual flow. Of course, the above description is simply a way of picturing the flow; it is not necessary to calculate the fictitious boundary to locate the shock, since the axial pressure distribution along the centerline can be computed. The method of calculating the shock position is outlined in the following sections.

SONIC ORIFICE

Consider an underexpanded flow issuing from a convergent nozzle, i.e., $M_N = 1$. The problem of exit Mach numbers other than one can be solved by a generalization of this case. The pressure variation along the centerline of such a flow has been calculated by Owen and Thornhill[6] for a total-pressure-to-atmospheric-pressure ratio, P_t/P_∞, of infinity. However, as pointed out by

Owen and Thornhill, the pressure variation thus calculated should hold for all P_t/P_∞ ratios "in that region bounded by the orifice and the first wave front which registers the existence of an external pressure outside the jet." Thus, for a considerable distance downstream, the pressure variation P/P_N, where P is the static pressure at a given point along the centerline and P_N is the static pressure at the nozzle exit, should be the same for all nozzle pressure ratios, P_t/P_∞, and as this pressure ratio increases, the region of similarity increases in size. Owen and Thornhill plotted P/P_N vs. x/d_N, where x is the distance downstream from the nozzle exit, and d_N is the exit diameter of the sonic nozzle (Fig. 2). They also plotted the Mach number at the centerline vs. x/d_N (Fig. 3). Using these graphs, a curve of P_2/P_N vs. x/d_N was plotted where P_2 is the pressure behind a shock, occurring at a Mach number corresponding to the given x/d (Fig. 2). It should be noted that the P/P_N curve calculated by Owen and Thornhill was continued past their maximum x/d_N of 3.85 so that P_2/P_N could be calculated. Since the curve of M vs. x/d_N (Fig. 3) was given up to $x/d_N = 10$, this could be done simply by finding the P/P_N corresponding to the Mach number at a given x/d_N. However, since the P/P_N curve is so close to a straight line for $x/d_N > 1.2$, and in view of the inaccuracies inherent in reading the original curves, a straight line extension was used, checking very well with calculations made from the Mach number curve.

The pressure behind the shock, P_2, was taken to be atmospheric (P_∞). Fig. 4 shows the results of such calculations for a range of $2 \leq P_N/P_\infty \leq 70$. This corresponds to a range of $3.8 \leq P_t/P_\infty \leq 133$ and a maximum total pressure of approximately 2000 psi if P_∞ is standard sea-level pressure. On the same graph, the experimental results obtained both at the NACA Langley Field Laboratories and at the Aircraft Propulsion Laboratory of The University of Michigan are plotted.* The error in x/d_N between the theoretical and the NACA

*The circles on the A.P.L. curve are actual experimental points; the NACA results are taken from curves drawn through their experimental points.

experimental curves is of the order of 12% to 14%, while the error between the A.P.L. experimental and the theoretical curve is less. The experimental setup for both laboratories is described in other reports,[7,8] so they will not be repeated in this paper, except to note that, at the NACA, Love and Grigsby took schlieren photographs while at the A.P.L., shadowgraphs were taken. This could certainly account for the difference between the two experimental curves. Furthermore, the absolute error between experimental and theoretical values of x, the distance from the nozzle to the Mach disc, is of the order 0.07 in., which is certainly of the order of the experimental error, the distances being measured on photographs. Therefore, the agreement between the theoretical and experimental curves appears to be most satisfactory, for the Mach one nozzle.

SUPERSONIC NOZZLES

For convergent-divergent nozzles with exit Mach numbers different from one, it is necessary to find the pressure distribution, if the same method is to be used. To visualize better the following arguments concerning the pressure distributions, a sketch of the flow out of an axisymmetric convergent-divergent nozzle is given in Fig. 5. For simplicity in this figure and succeeding figures, only half the flow field is shown, and none of the intersection waves is drawn, although their effect is pictured through the curvature of the waves shown. The lines a-b, a-c, etc., are the wave fronts emanating from the expansion around the nozzle lip. a-b, in particular is the Mach line defined by the wave angle, $\mu = \sin^{-1} 1/M_N$, i.e., it is the first wave in the expansion fan. It is apparent, from this picture, that, along the centerline, the fluid can be outside the nozzle, and still be at M_N, the exit Mach number of the nozzle. That is, until the centerline fluid reaches b, no expansion signals reach it. However, after b, the centerline receives signals from a, which correspond to various Mach numbers at a, as the flow turns the corner. Again, the structure

along the centerline should be the same for all total-pressure-to-atmospheric-pressure ratios until the wave front signaling the exterior pressure reaches the centerline. That is, the same argument holds for the centerline flow downstream from point b for the nozzle where $M_N > 1$ as holds for the centerline flow downstream from the nozzle edge for the nozzle where $M_N = 1$. However, as M_N changes, the distance from the nozzle to b changes and must be accounted for. Thus the problem is essentially that of finding the pressure distribution downstream from point b. However, it is hypothesized that the desired pressure distribution can be found from the pressure distribution behind a $M_N = 1$ nozzle (sonic orifice). The arguments supporting this hypothesis are as follows.

Consider again the flow behind a $M_N = 1$ nozzle (Fig. 6). As the expansion waves from the corner at a_1 intersect the centerline, the flow is expanded so that a variation of Mach number exists. In fact, at a point b_1, say, the Mach number is the same as the Mach number in the flow behind a $M_N > 1$ nozzle, at point b. Furthermore, at point a_1, as the flow turns through an angle greater than that corresponding to the expansion wave a_1-b_1, it expands through the same Mach numbers, and thus passes through the same expansion waves as does the flow in Fig. 5, expanding beyond the line a-b. These waves propagate to the centerline in both cases, causing a variation in pressure and Mach number, etc. This means that, as shown in Figs. 5 and 6, there is a region on the centerline of both flows (b_1-d_1 and b-d, say) where the same expansion takes place. The lengths b_1-d_1 and b-d are very nearly the same, unless the Mach number of the nozzle, M_N, in the case where M_N is different from one, is very high, when the initial angles of inclination of the lines a-b and a_1-b_1, ω and ω_1, respectively, are very small. Then a small difference in starting angle, at a, and a_1, for any later expansion wave, means a large difference in distance traversed on the centerline. The starting angles at a and a_1 for any of the expansion waves are different, of course, because in the $M_N > 1$ nozzle the flow cor-

responding to the line a-b is parallel to the axis, while in the $M_N = 1$ case, the flow corresponding to line a_1-b_1 is at an angle to the axis, depending on the value of the Mach number associated with this line.

The result of the above arguments is, then, that it is assumed that, for $M_N > 1$, the pressure distribution for $x > x_b$ is the same as the pressure distribution for the $M_N = 1$ nozzle flow for $x > x_{b_1}$. For a flow behind a nozzle with exit Mach number of $M_N = 2$, for example, b_1 is located at that point where the centerline Mach number is 2. Furthermore, since the assumption is again made that the shock occurs so that the static pressure behind it is atmospheric, the distance from b_1 to the Mach disc in $M_N = 1$ flow is the same as the distance from b to the Mach disc in $M_N = 2$ flow, for the same total-to-atmospheric-pressure ratio, P_t/P_∞.

To describe analytically the above arguments, the following dimensionless notation is used:

$$
\begin{aligned}
\xi_1 &= (x_m/d_N)_{M_N=1} \\
\xi_{b_1} &= (x_{b_1}/d_N)_{M_N=1} \\
\Delta\xi_1 &= [(x_m - x_{b_1})/d_N]_{M_N=1} \\
\xi &= (x_m/d_N)_{M_N} \\
\xi_b &= (x_b/d_N)_{M_N} \\
\Delta\xi &= [(x_m - x_b)/d_N]_{M_N}
\end{aligned}
\tag{1}
$$

where x_m is the distance from the nozzle to the Mach disc, and x_b and x_{b_1} are the distances between the nozzles and the points b and b_1, respectively. d_N is the exit diameter of either the sonic or supersonic nozzle depending on whether it is used in ξ_1 or ξ. Point b is the point in the supersonic nozzle

flow where the first wave of the expansion fan intersects the centerline, and point b_1 is the point on the sonic nozzle flow centerline where the Mach number reaches the value of the exit Mach number of the supersonic nozzle in question. For any given P_t/P_∞, ξ_1 is a known quantity, found by the use of Fig. 2. Furthermore, for a given supersonic nozzle, i.e., for a given M_N, ξ_{b_1} can be found from Fig. 3. Finally, knowing ξ_1 and ξ_{b_1} one can find $\Delta\xi_1$, since

$$\Delta\xi_1 = \xi_1 - \xi_{b_1} \quad . \tag{2}$$

Next, ξ_b depends on μ, the Mach angle associated with M_N.

$$\xi_b = [2 \tan \mu]^{-1}. \tag{3}$$

The value of $x_m - x_b$ is the same as $x_N - x_{b_1}$, but to compute $\Delta\xi_b$, $\Delta\xi_{b_1}$ must be corrected to the exit diameter equivalent to the M_N of the supersonic nozzle. Thus,

$$\Delta\xi_b = \Delta\xi_{b_1} \cdot \frac{(d_N)_{M_N=1}}{(d_N)_{M_N}}$$

$$= \Delta\xi_{b_1} \left[\left(\frac{A^*}{Ae}\right)_{M_N}\right]^{1/2} \quad . \tag{4}$$

Then, one can write the equation for ξ as

$$\xi = \Delta\xi_{b_1} \left[\left(\frac{A^*}{Ae}\right)_{M_N}\right]^{1/2} + \frac{1}{2 \tan \mu} \quad , \tag{5}$$

where $\Delta\xi_{b_1}$ and ξ are calculated at the same P_t/P_∞.

Eq. (5) was used to calculate the curves shown in Figs. 7a, b, c, and d, and the experimental values were also plotted for comparison. As in the case of $M_N = 1$, the comparison with experiment is quite good. Of course, the comparison between theory and experiment is made better by the fact that at low exit Mach numbers the theoretical curve predicts values which are larger than experimental, while as the Mach number increases, the difference becomes less

at first and then increases so that the theoretical curve predicts values less than experimental curves. If the experimental values at $M_N = 1$ were used for ξ_1, the error at higher Mach numbers would be considerably greater.

It should be mentioned that several tests were carried out with various nozzle divergence half angles (δ_N), but the effect of nozzle divergence on the position of the first Mach disc was negligible, except perhaps at the higher nozzle Mach numbers where the effects were still relatively quite small.

CALCULATION OF THE JET BOUNDARY

The ideal fluid jet boundary can be calculated using characteristic theory.[9,10] This gives a good approximation to the real jet boundary, although there is actually a viscous mixing region along the boundary. However, the work involved for each nozzle and pressure ratio is considerable and is still only approximate for the above reason and because there is some question about continuation of the characteristic net beyond the intercepting shock. Therefore, the following method is presented as a relatively quickly calculated approximation to the initial jet boundary. It does not agree with experimental photographs as well as the solutions obtained by the method of characteristics. However, the difference between the two becomes significant only at the higher jet expansion angles. At relatively low expansion angles, the agreement is quite good.

Consider the flow at the lip of a nozzle (Fig. 8) with half angle δ_N. At the nozzle lip, before expansion, the Mach number is M_N, and the corresponding Prandtl-Meyer angle is ν_N. After expanding to atmospheric pressure, the Mach number is M_e with a corresponding Prandtl-Meyer angle of ν_e. Thus, the flow at the nozzle lip turns through an angle of $\nu_e - \nu_N$ relative to the nozzle wall, and the overall flow expansion angle with respect to the flow axis is α, where

$$\alpha = \nu_e - \nu_N + \delta_N \quad . \tag{6}$$

The flow is turned from this initial expansion angle by the intersection of expansion waves with the boundary, reflecting as compression waves, so that the condition of constant pressure on the boundary is satisfied at every point. However, the present approximation depends on replacing the effects of expansion waves intersecting the flow near the boundary, by the effects of a quasi-one-dimensional area increase. That is, just as in one-dimensional nozzle flow, it is assumed that one can find the average Mach number and pressure at any axial position in an expanding flow from the area ratio at the given point, instead of going through a characteristic calculation.

Immediately after leaving the nozzle exit, then, the flow at the lip has turned through the total angle α. However, as it follows this new direction, it is continually expanding. Hence, in an incremental distance downstream, dx, there is an increase in area, dA, with a corresponding decrease in pressure, $\partial P/\partial A \cdot dA$. $\partial P/\partial A$ can be calculated from quasi-one-dimensional relations if one considers a stream tube along the boundary of the jet to be the channel in question. Since a change in pressure along the jet boundary cannot be tolerated, this decrease in pressure must be balanced by an equivalent increase in pressure which can only be gained by turning the flow through an incremental angle, $d\theta$, thus forming a weak compression wave. This process of expansion and compression holds at any point on the boundary where at x, with a given r, and a given direction of flow, θ (Fig. 9), the gas in expanding in this given direction to $r + dr$ at $x + dx$ would undergo a decrease in pressure so that a further change in direction, $d\theta$, results, keeping the pressure at a constant level at $r + dr$.

The equation for the pressure along the jet boundary may then be written as follows:

$$dP = 0 = \frac{\partial P}{\partial A} dA + \frac{\partial P}{\partial \theta} d\theta \quad . \tag{7}$$

Since a change in area, dA, is equivalent to a change in Mach number, dM, Eq. (7) can be written in terms of M and θ. Thus,

$$\frac{\partial P}{\partial M} dM + \frac{\partial P}{\partial \theta} d\theta = 0 \quad , \tag{8}$$

where $\partial P/\partial M$ is calculated from isentropic flow relation.

Next, if $p = P/P_t$, where P_t is the total pressure for the flow along the jet boundary, then Eq. (8) becomes

$$\frac{\partial p}{\partial M} dM + \frac{\partial p}{\partial \theta} d\theta = 0 \quad . \tag{9}$$

P_t is assumed constant along the boundary, since the waves are of infinitesimal strength.

For isentropic flow, p is related to M as follows:

$$p = [1 + (\gamma-1)M^2/2]^{-\gamma/(\gamma-1)} \tag{10}$$

so that

$$(\partial p/\partial M)\, dM = (\partial p/\partial M^2)\, dM^2 = -\gamma/2 \frac{p\, d\, M^2}{\left(1 + \frac{\gamma-1}{2} M^2\right)} \tag{11}$$

From linearized theory, the change in pressure due to a small change in direction is

$$\Delta P = \frac{\gamma P M^2}{\sqrt{M^2 - 1}} \Delta\theta \quad . \tag{12}$$

Hence, in terms of a vanishingly small change in pressure and direction,

$$\partial p/\partial \theta = \frac{\gamma p M^2}{\sqrt{M^2 - 1}} \quad . \tag{13}$$

Substituting Eqs. (11) and (13) in (9), one obtains the following relation between θ, the angle measured from the original direction of boundary flow at

the nozzle exit, and M, the Mach number at any point along the boundary:

$$-\gamma/2 \frac{p}{\left(1 + \frac{\gamma-1}{2} M^2\right)} dM^2 + \frac{\gamma\, p\, M^2}{\sqrt{M^2 - 1}} d\theta = 0 \quad . \tag{14}$$

Substituting $\beta = \sqrt{M^2-1}$ into Eq. (14) and rearranging, one obtains

$$d\theta = \frac{2}{(\gamma-1)} \frac{\beta^2}{(\beta^2+1)} \left(\frac{\gamma+1}{\gamma-1} + \beta^2\right)^{-1} d\beta \quad . \tag{15}$$

Eq. (15) can be integrated now, from the nozzle-exit conditions after expansion, to any point on the boundary. At the nozzle exit, $\beta = \beta_e$ ($M = M_e$) and $\theta = 0$. Thus,

$$\theta = \sqrt{\frac{\gamma+1}{\gamma-1}} \tan^{-1}\left(\sqrt{\frac{\gamma-1}{\gamma+1}}\,\beta\right) - \tan^{-1}\beta - \left\{\sqrt{\frac{\gamma+1}{\gamma-1}} \tan^{-1}\left(\sqrt{\frac{\gamma-1}{\gamma+1}}\,\beta_e\right) - \tan^{-1}\beta_e\right\}. \tag{16}$$

Hence, with the given approximations, Eq. (16) indicates that for the condition of constant pressure to hold, the turning angle, θ, at any point, is simply the difference between the Prandtl-Meyer angle associated with the Mach number corresponding to the area ratio at that point and the Prandtl-Meyer angle associated with the Mach number, M_e.

With θ known, one can calculate the jet boundary in terms of r and x, since if ψ is the angle made by the tangent to the jet boundary with the axis, then (Fig. 9)

$$\tan\psi = \frac{dr}{dx} \quad . \tag{17}$$

But

$$\psi = \alpha - \theta \quad , \tag{18}$$

and if one defines a dimensionless r and x, in terms of the radius of the exit section of the nozzle, then Eq. (17) can be written as,

$$d(x/r_N) = \frac{d(r/r_N)}{\tan(\alpha-\theta)} \quad . \tag{19}$$

Hence, x/r_N at any point (where x = 0 at the nozzle exit) is as follows:

$$\frac{x}{r_N} = \int_1^{r/r_N} \frac{d\,(r/r_N)}{\tan\,(\alpha-\theta)} \quad . \tag{20}$$

The integral in Eq. (20) may be calculated numerically, using Simpson's rule of integration. At any $\frac{r}{r_N}$, the corresponding area ratio (A/A^*) may be calculated, using as $(A/A^*)_{\frac{r}{r_N}=1}$ the value which corresponds to M_e. Thus,

$$(A/A^*)_{\frac{r}{r_N}} = \left(\frac{r}{r_N}\right)^2 (A/A^*)_{M=M_e} \quad .$$

Knowing the area ratio, the Mach number and θ can be found from compressible flow tables. For any given set of nozzle parameters, α can be calculated using Eq. (6).

In Figs. 10a, b, and c, plots of r vs. x are given for nozzle angles of $\delta_N = 0$ for various P_N/P_∞, when M_N = 1, 2, and 3. On the same graphs are plotted the characteristic solutions reported by Love and Grigsby.[11]

It is clear that this approximation is good only when the angle which the jet boundary makes with the axis at the nozzle lip is relatively small, i.e., at relatively low pressure ratios, P_N/P_∞. Furthermore a nozzle Mach number effect exists. At Mach number, M_N = 1.0, for example, the maximum percentage difference, based on the characteristic solution, goes from 5% at P_N/P_∞ = 2, where P_t/P_∞ = 3.8, to 9% at P_N/P_∞ = 20, when $P_t/P_\infty \cong 80$. At M_N = 3, however, this percentage difference is 16% at P_N/P_∞ = 2, where $P_t/P_\infty \cong 74$, and 29% even at P_N/P_∞ = 10, where $P_t/P_\infty \cong 370$. Hence, the approximation is limited by pressure ratio and nozzle Mach number, depending on the accuracy desired.

To give some idea of the comparison between these calculations and experiment, the calculated curves have been drawn on the experimental photographs in Figs. 11a through e. In each case the pressure ratios of both the experiment and the theoretical calculations agreed within a few percent. Again, at relatively low pressure ratios, the agreement is quite good, while at very high

pressure ratios it is quite inaccurate.

It should be noted that, with the approximate method of calculating the inviscid jet boundary, only the diverging part of the flow can be considered. Thus, as $\psi \to 0$, i.e., as the jet boundary tends to become parallel to the axis, $x \to \infty$, since $1/\tan \to \infty$. This restriction was pointed out also by Love[12] in a recent note in which he used a similar method to calculate the boundary between two supersonic streams with different Mach numbers and pressures.

CONCLUSIONS

A method for calculating the position of the first normal shock in the jet flow behind highly underexpanded nozzles has been found. It gives good results when compared to experimental results, for a range of pressure ratios of $5 \leq P_t/P_\infty \leq 140$ and for range of nozzle exit Mach numbers of $1 \leq M_N \leq 3$.

The approximate method presented for calculating the boundary of a supersonic jet exhausting into an atmosphere at rest is much easier to apply than a characteristic solution. However, its validity is limited by the accuracy desired to relatively low nozzle-exit-to-atmospheric-pressure ratios, and relatively low supersonic Mach numbers at the nozzle exit.

REFERENCES

[1]Love, Eugene S., and Grigsby, Carl E., Some Studies of Axisymmetric Free Jets Exhausting from Sonic and Supersonic Nozzles into Still Air and into Supersonic Streams, NACA, RML54L31, 1955.

[2]Prandtl, L., Über die stationären Wellen in einem Gasstrahle, Physik Z., Vol. 5, pp. 599-601, 1904; also, Neue Untersuchungen über die strömende Bewegung der Gase und Dämpfe, Physik Z., Vol. 8, pp. 23-32, 1907.

[3]Love and Grigsby, p. 10.

[4]Ibid.

[5]Wilcox, Donald E., Weir, Alexander, Nicholls, James A., and Dunlap, Roger, Location of Mach Discs and Diamonds in Supersonic Air Jets, Journal of the Aeronautical Sciences, Vol. 24, No. 2, pp. 150-152, February, 1957.

[6]Owen, P. L., and Thornhill, C. K., The Flow in an Axially-Symmetric Supersonic Jet from a Nearly Sonic Orifice into a Vacuum, Brit., A.R.C. Technical Report, R and M 2616, 1952.

[7]Love and Grigsby.

[8]Wilcox et al.

[9]Kelber, C. N., and Jarvis, S., An Analysis of the Gas Flow from a Very High Pressure Nozzle, Frankfort Arsenal Report No. R-1107, December, 1952.

[10]Love and Grigsby.

[11]Ibid.

[12]Love, Eugene S., An Approximation of the Boundary of a Supersonic Axisymmetric Jet Exhausting into a Supersonic Stream, Journal of the Aeronautical Sciences, Vol. 25, No. 2, p. 130, February, 1958.

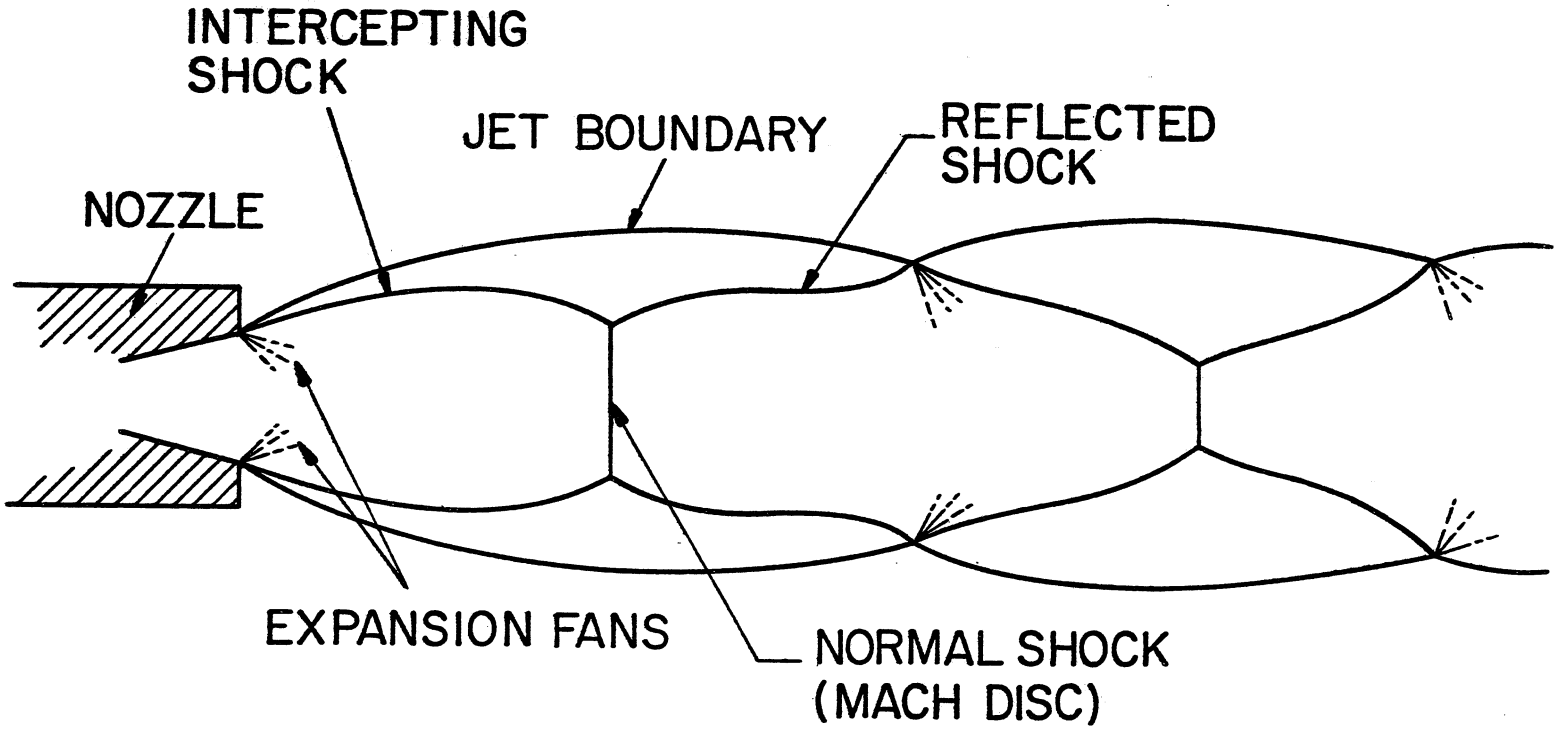

Fig. 1. Sketch of jet structure behind a highly underexpanded nozzle.

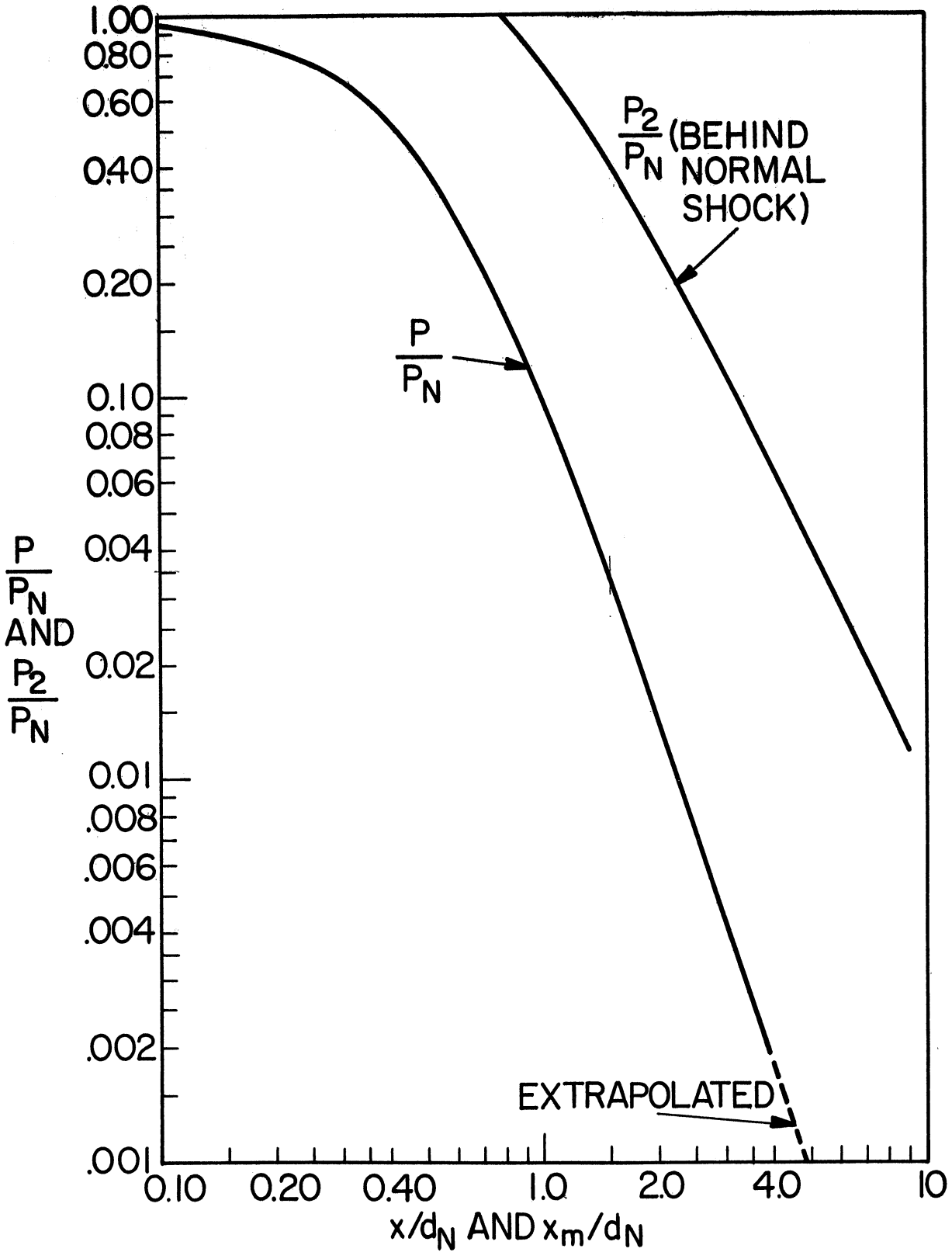

Fig. 2. Variation of the pressure, and the pressure behind a normal shock at the same axial position, along the centerline of the flow from a sonic orifice into a vacuum (axial pressure distribution after Owen and Thornhill, reference 6).

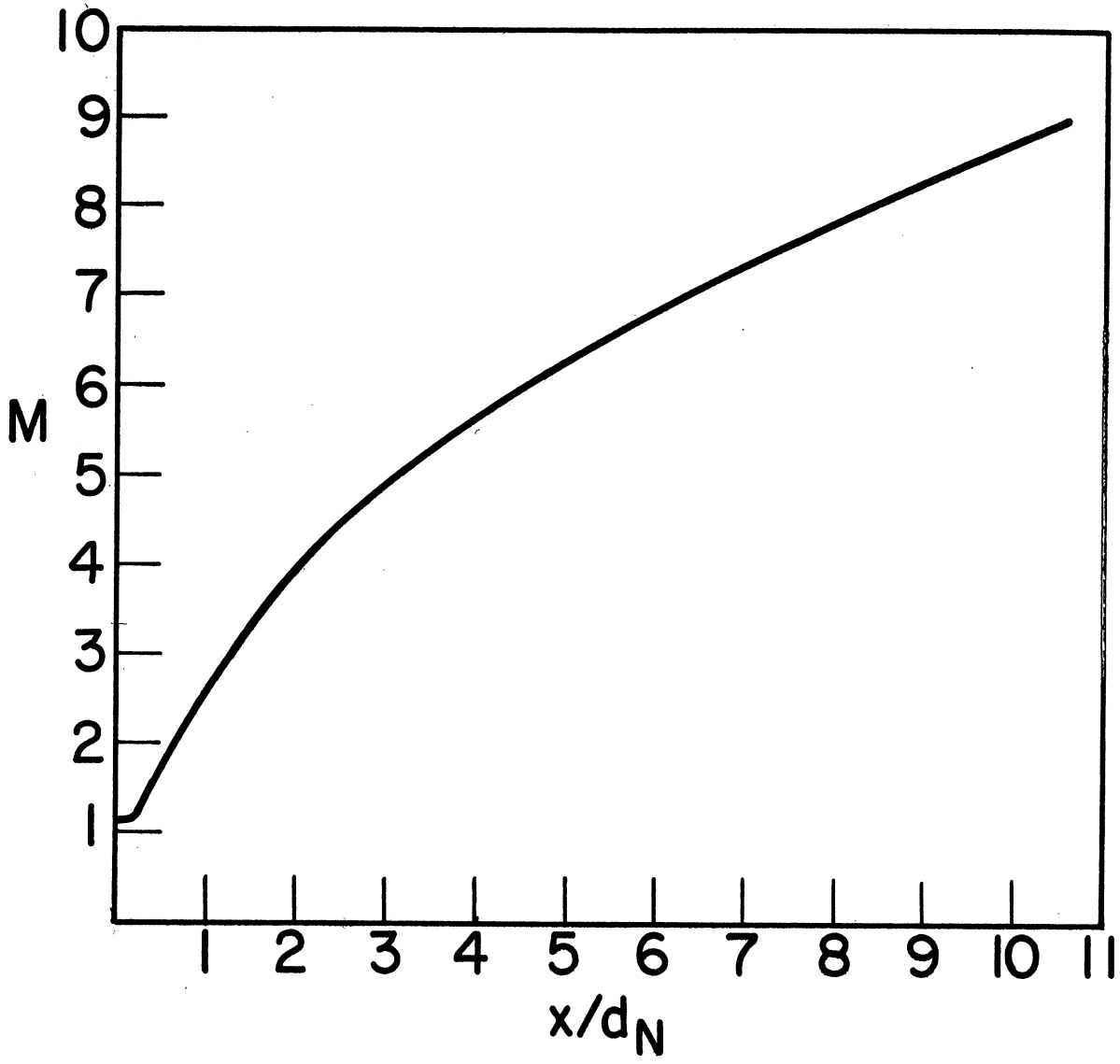

Fig. 3. Axial variation of Mach number along the centerline of the flow from a sonic orifice into a vacuum (after Owen and Thornhill, reference 6).

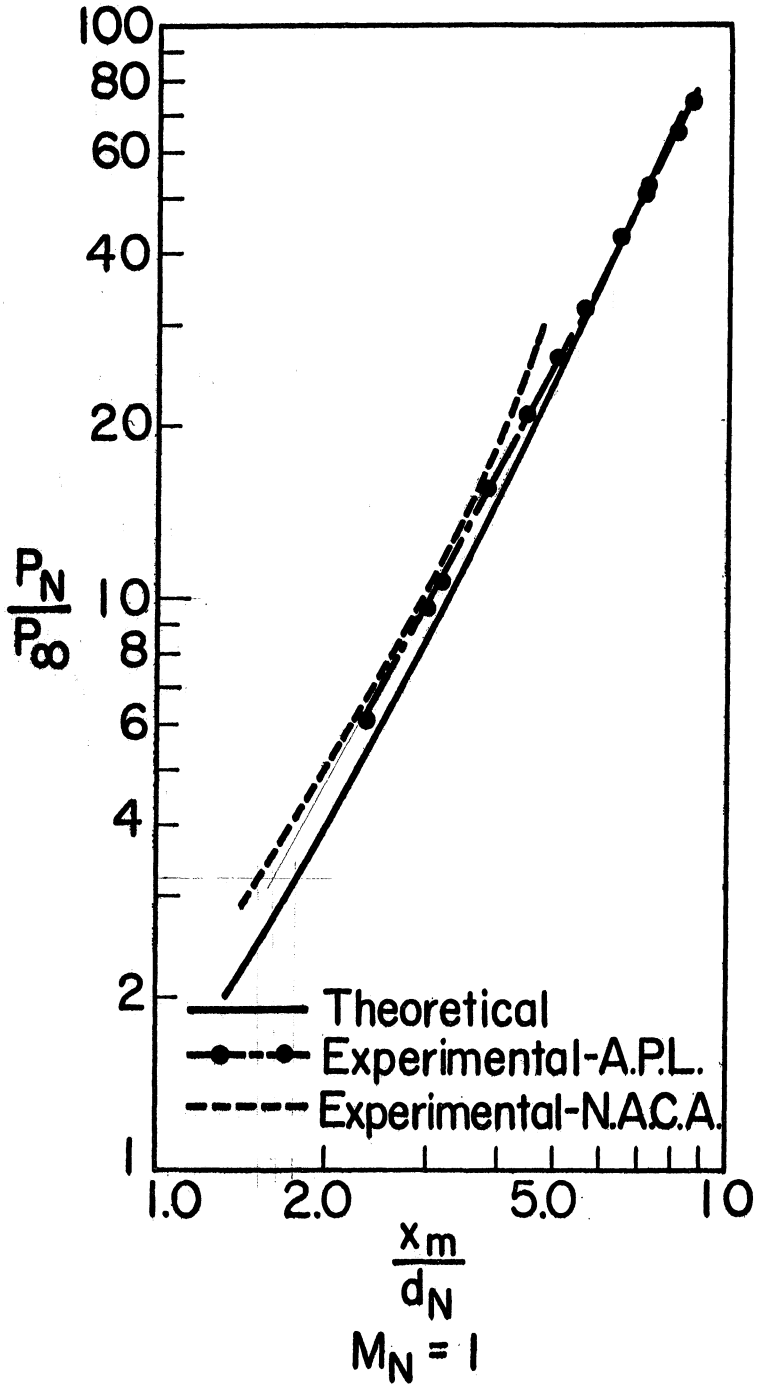

Fig. 4. Variation of the distance between the nozzle exit and the first normal shock (Mach disc) with the pressure at the nozzle exit for a sonic nozzle.

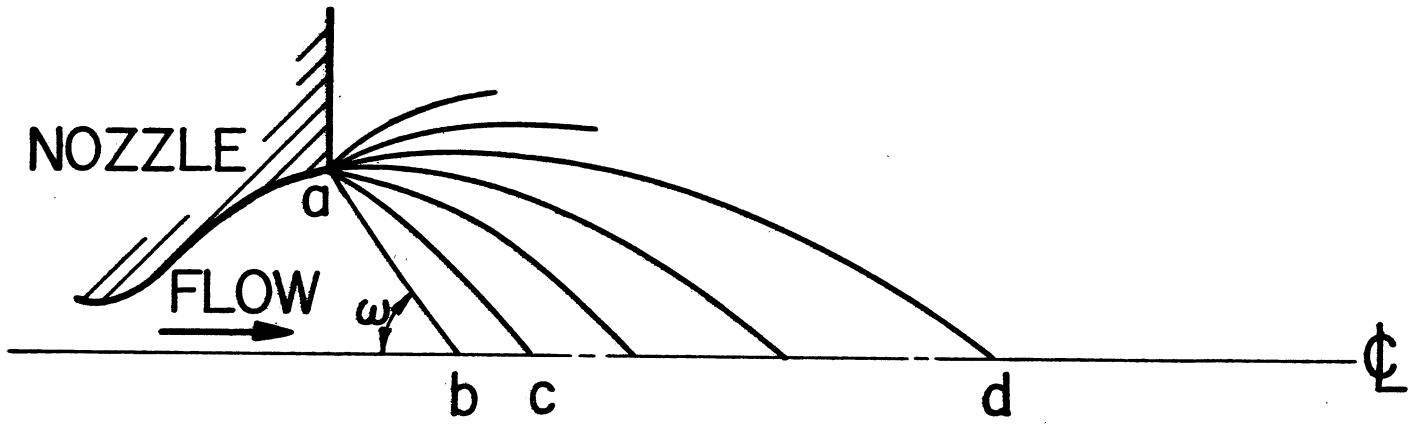

Fig. 5. Sketch of expansion waves emanating from the corner of an underexpanded nozzle with $M_N > 1$.

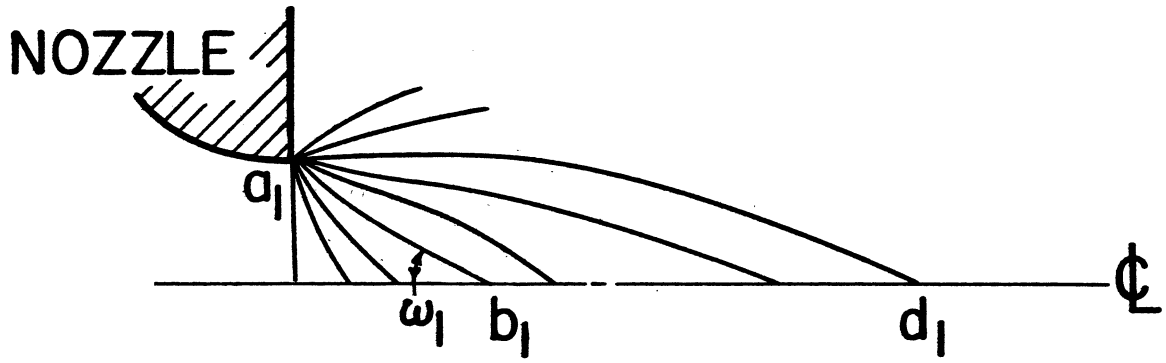

Fig. 6. Sketch of expansion waves emanating from the corner of an underexpanded sonic orifice.

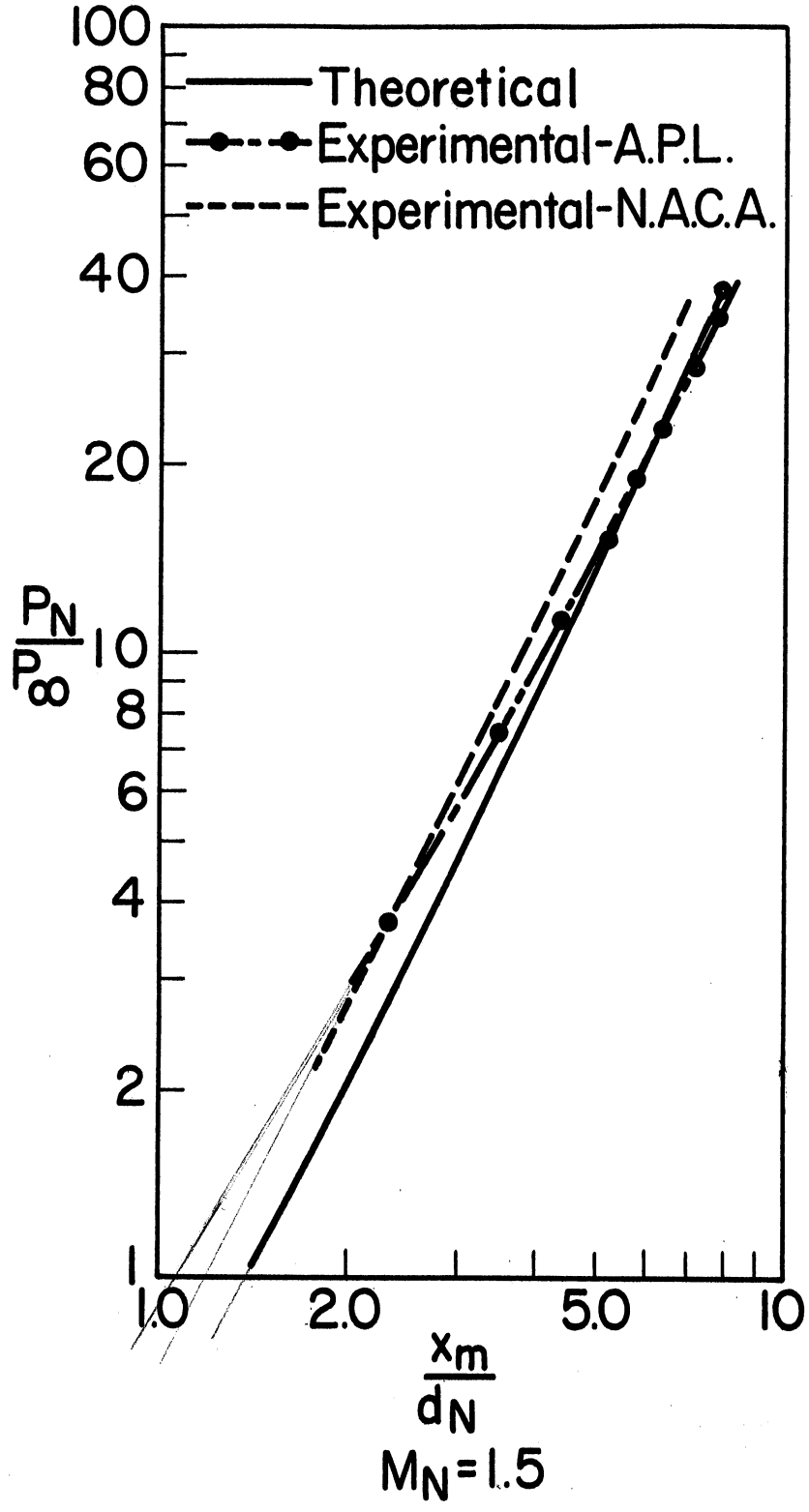

(a)

Fig. 7. Variation of the distance between the nozzle exit and the first normal shock (Mach disc) with the pressure at the nozzle exit for nozzles with supersonic exit Mach numbers.

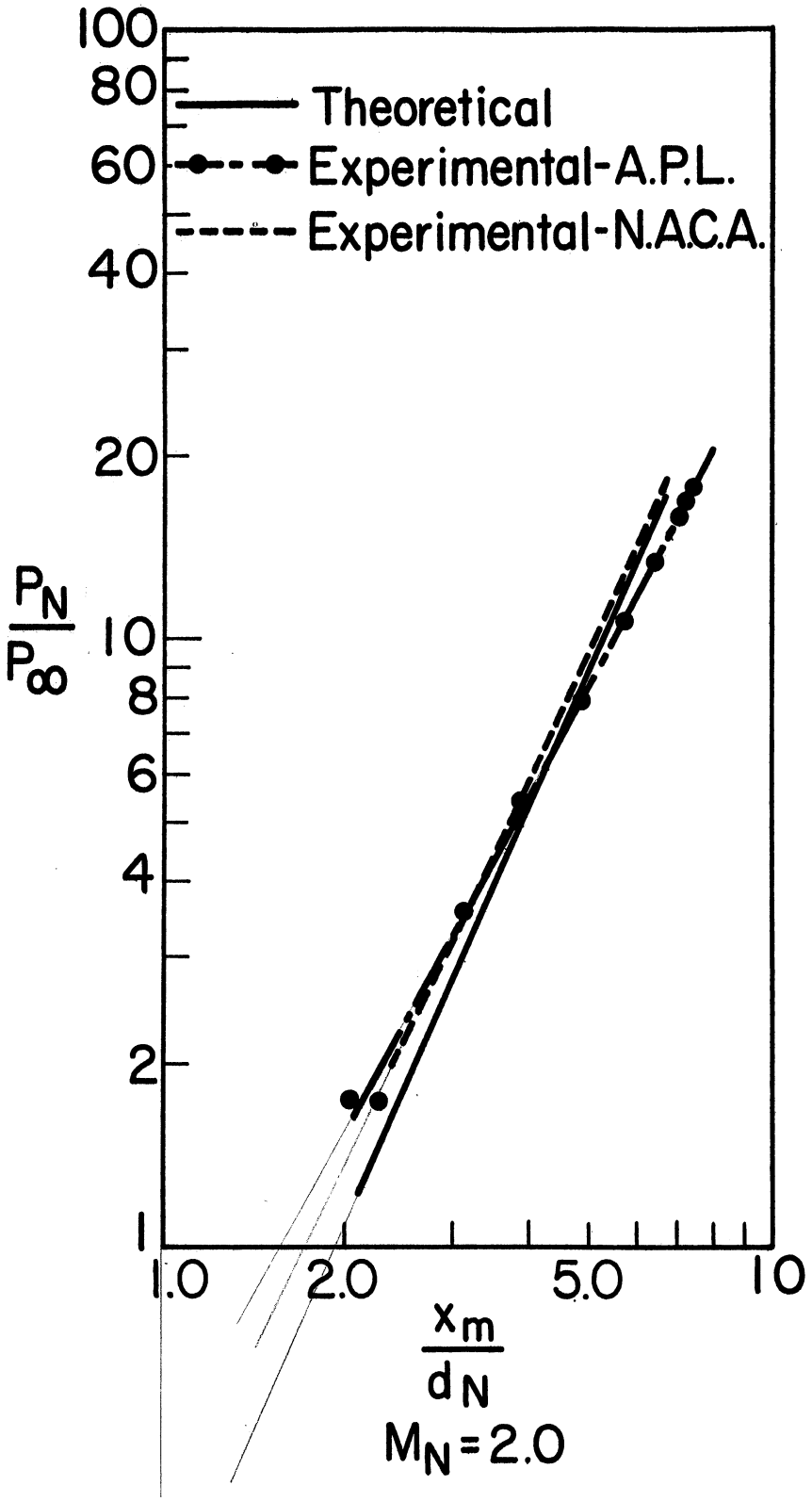

(b)

Fig. 7. Continued.

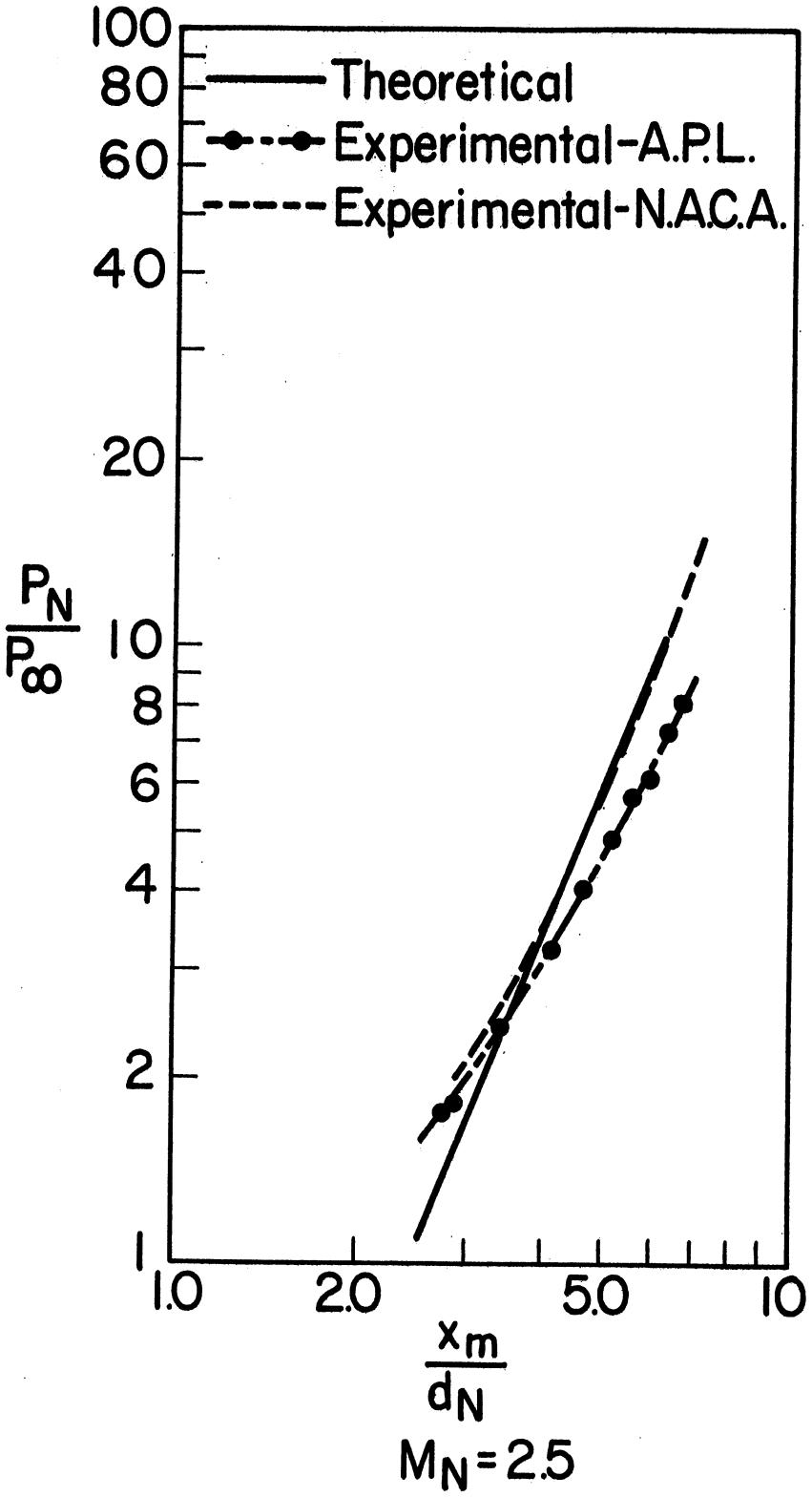

(c)

Fig. 7. Continued.

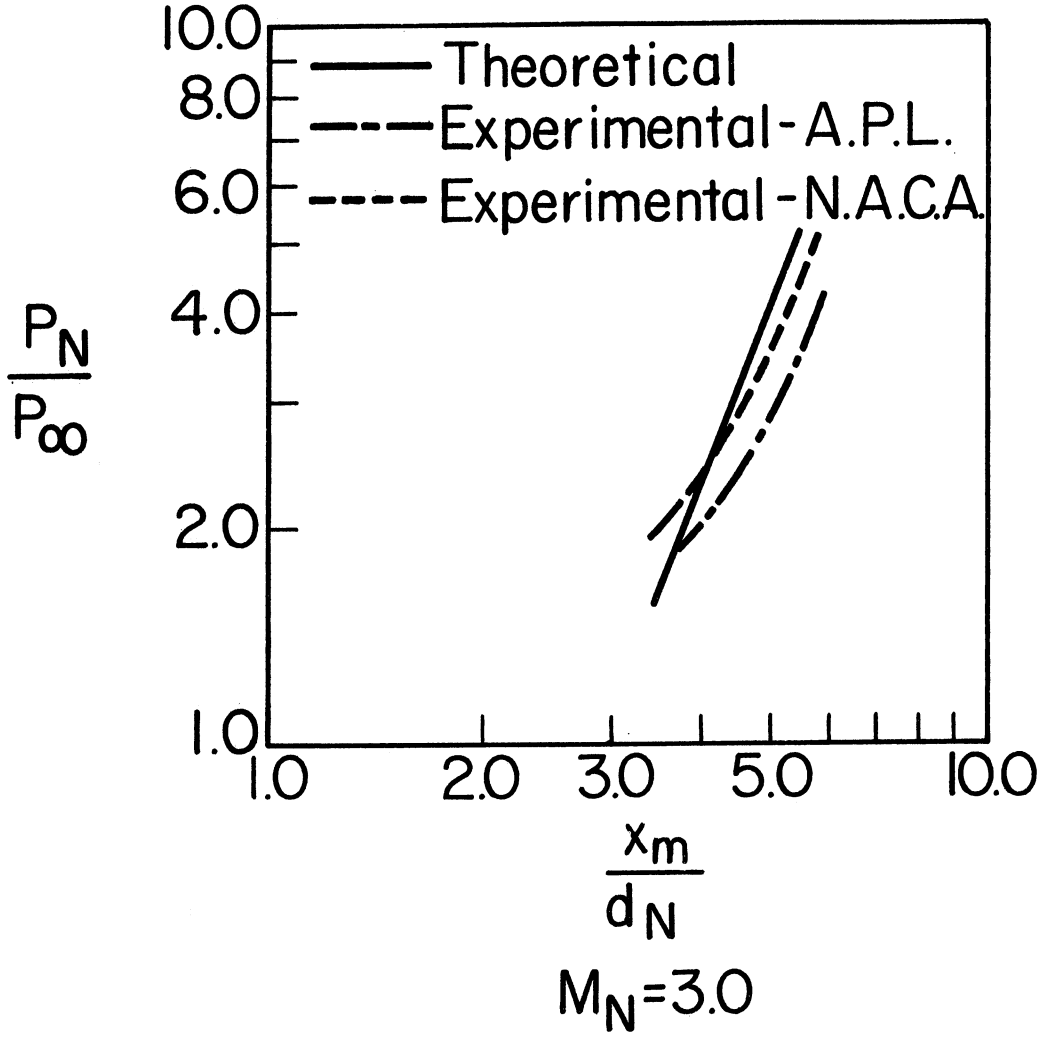

(d)

Fig. 7. Concluded.

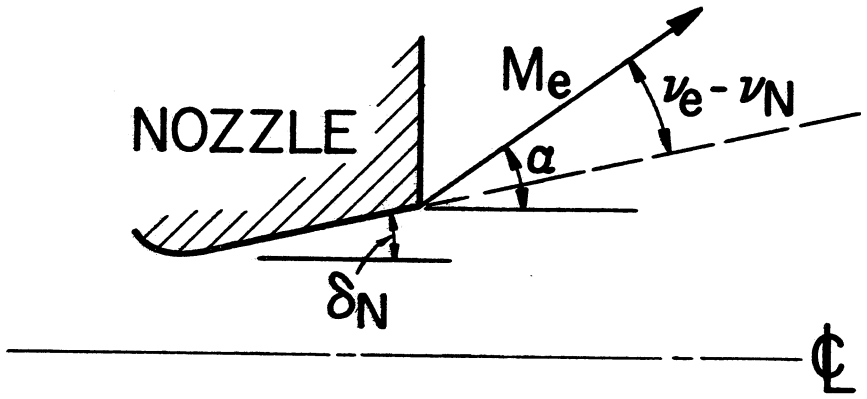

Fig. 8. Total angle turned through by the flow at the lip of an underexpanded nozzle, in terms of nozzle half angle and Prandtl-Meyer turning angles.

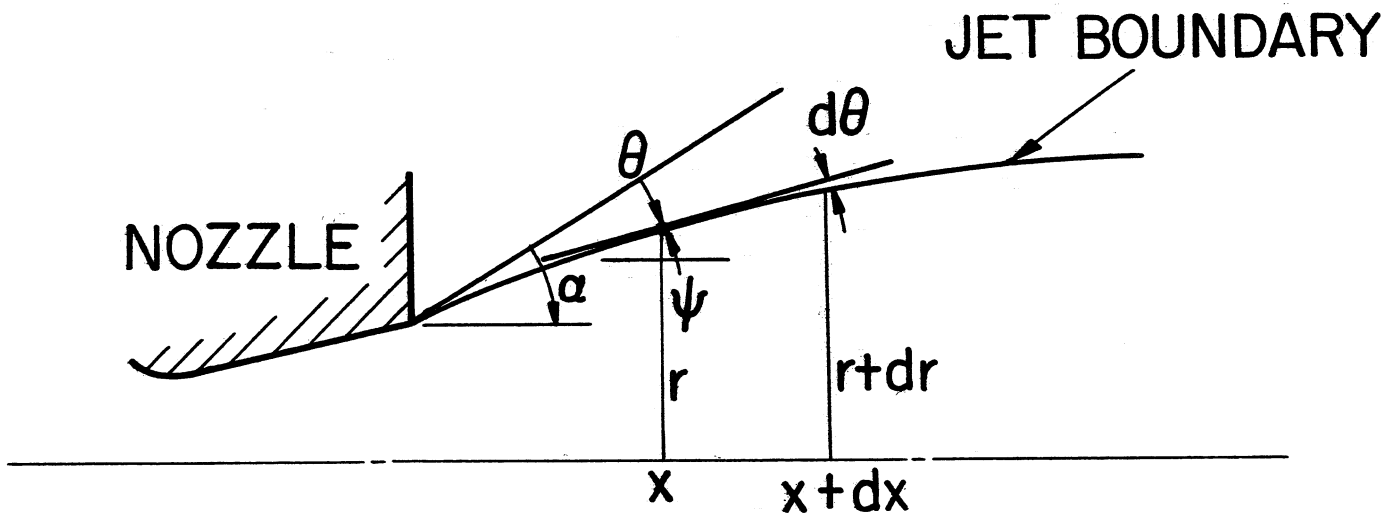

Fig. 9. Incremental angle and radius changes in the jet boundary due to an incremental increase in x, the axial coordinate.

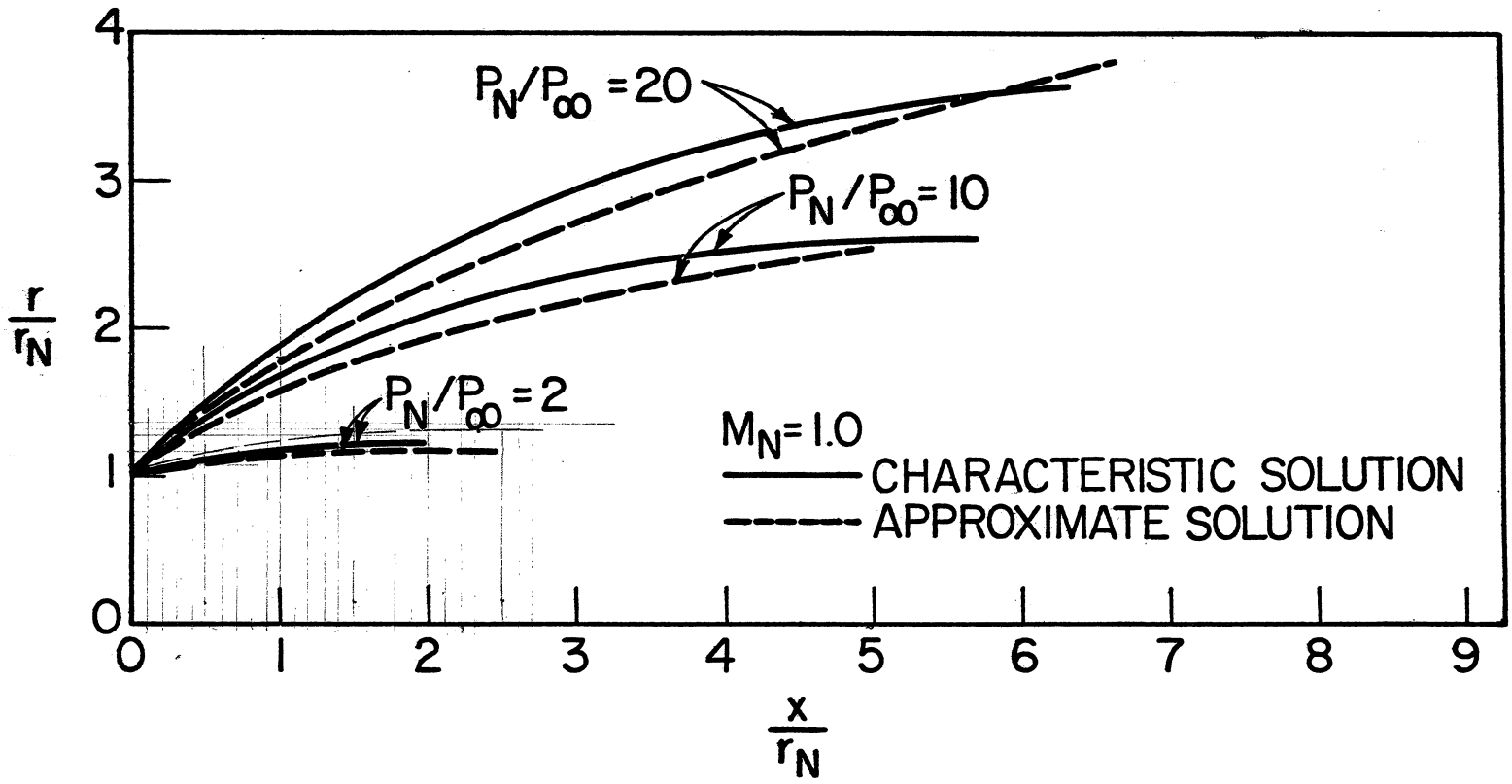

(a)

Fig. 10. Comparison of jet boundaries calculated by approximate method with those calculated by the method of characteristics for sonic and supersonic nozzles with various pressure ratios.

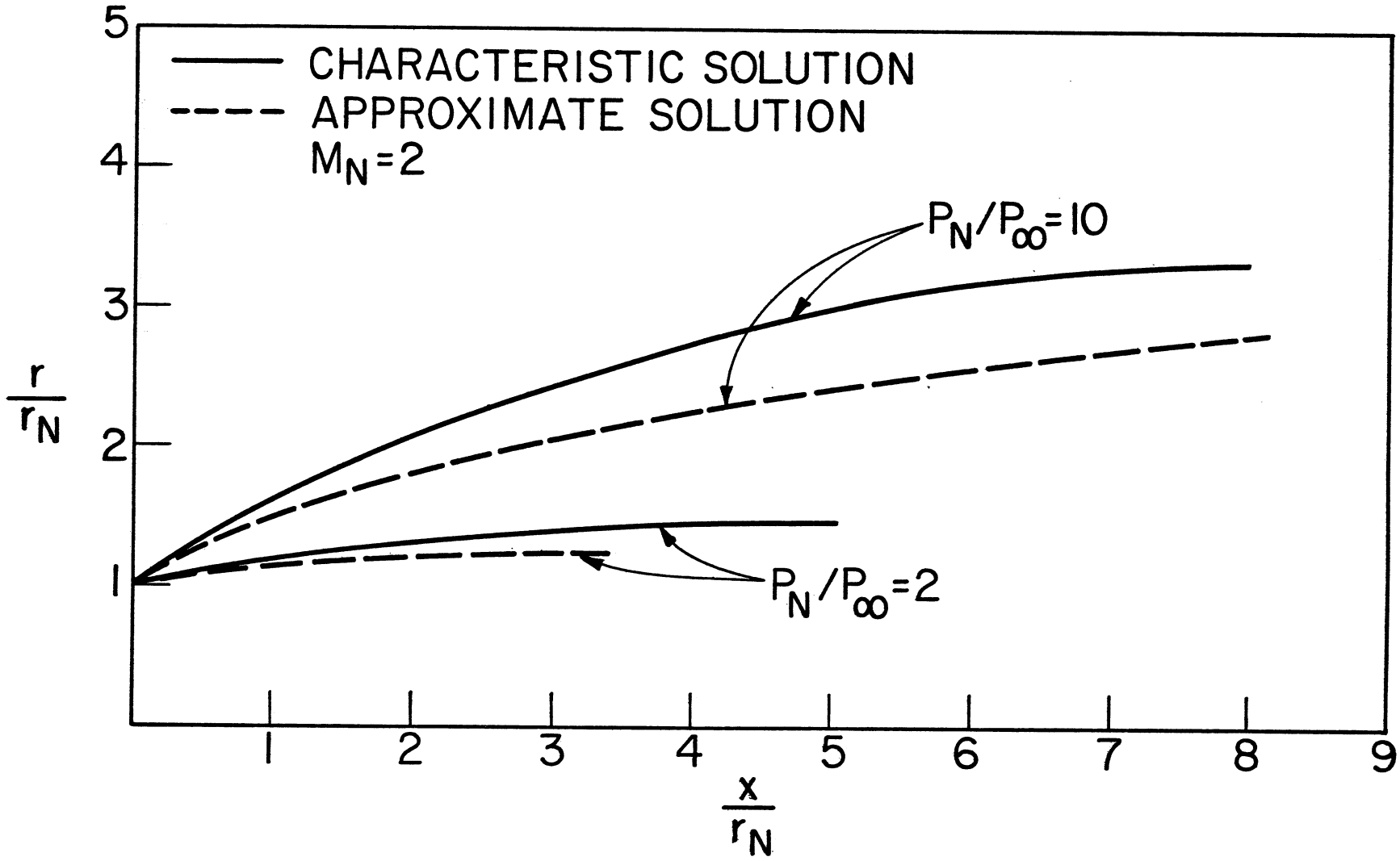

(b)

Fig. 10. Continued.

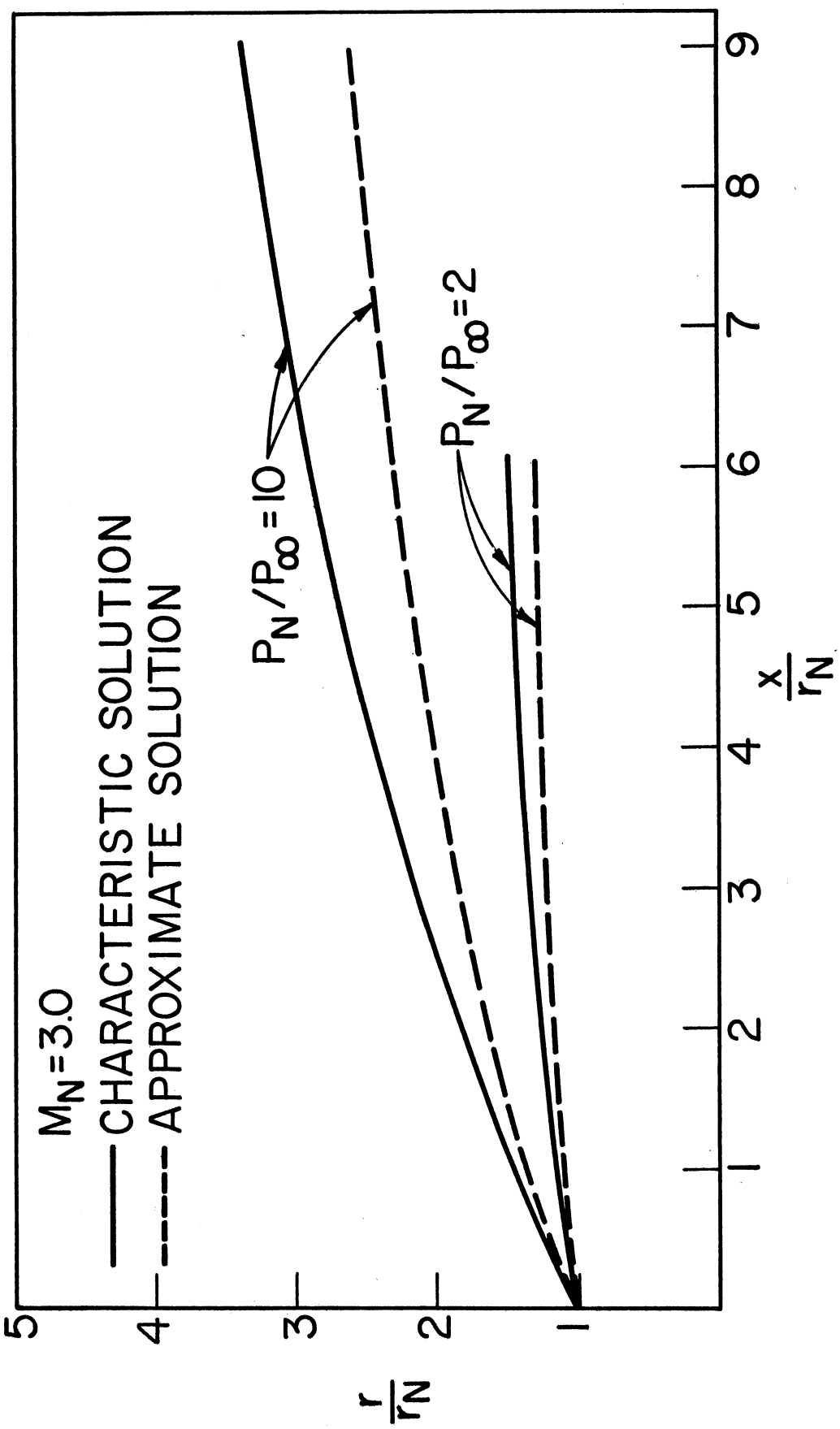

(c)

Fig. 10. Concluded.

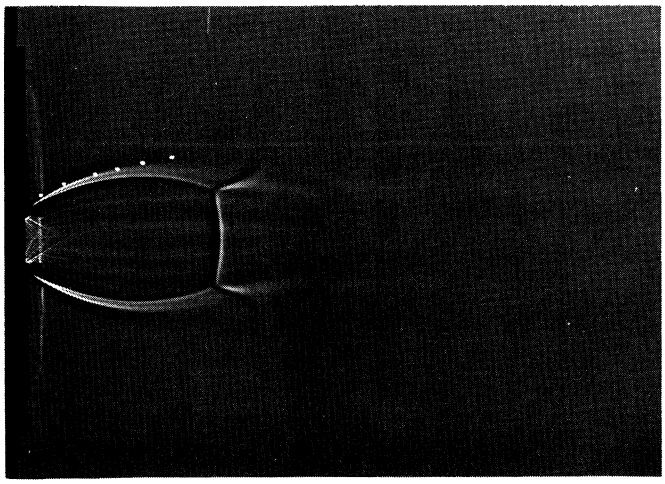

a. $M_N = 1$, $P_t/P_\infty = 18.5$, $P_N/P_\infty = 9.77$

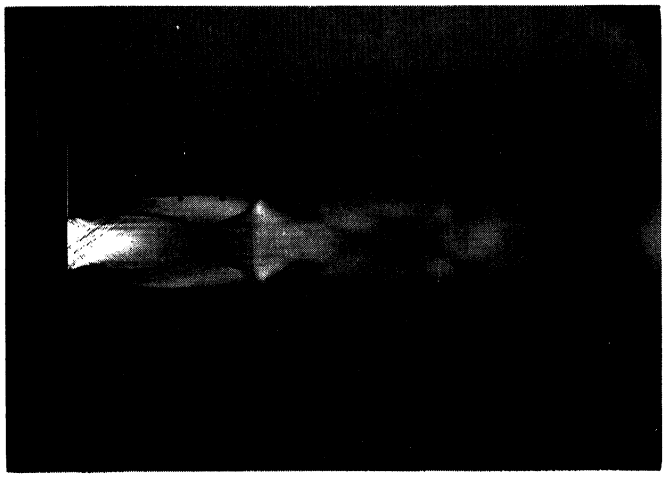

b. $M_N = 2$, $\delta_N = 10°$, $P_t/P_\infty = 24.6$, $P_N/P_\infty = 3.14$

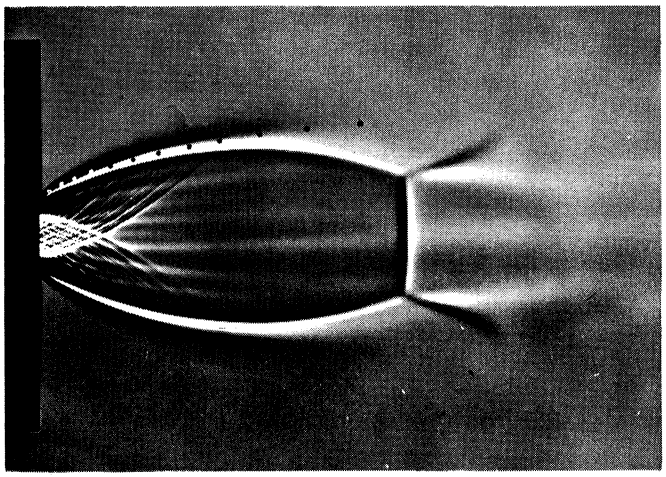

c. $M_N = 2$, $\delta_N = 10°$, $P_t/P_\infty = 62.2$, $P_N/P_\infty = 7.95$

Fig. 11. Comparison of approximate jet boundaries with the boundaries seen on a shadowgraph.

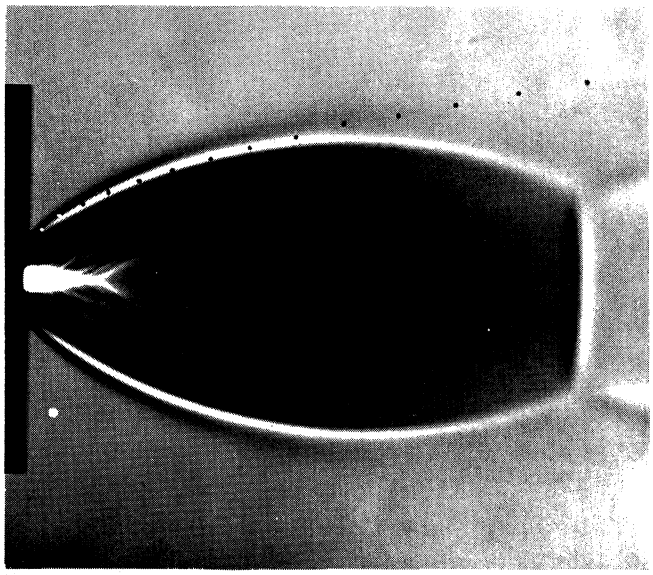

d. $M_N = 2$, $\delta_N = 10°$, $P_t/P_\infty = 138.7$, $P_N/P_\infty = 17.7$

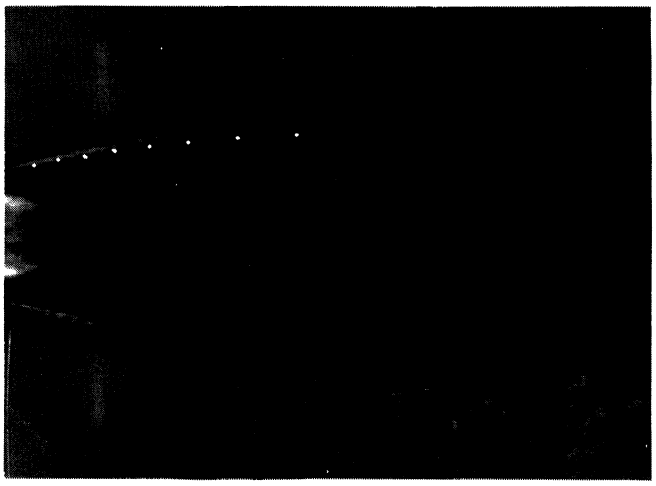

e. $M_N = 3$, $\delta_N = 10°$, $P_t/P_\infty = 139.5$, $P_N/P_\infty = 3.80$

Fig. 11. Concluded.

DISTRIBUTION LIST
Contract No. DA-20-018-ORD-13821

Agency	Copy
Commanding Officer Office of Ordnance Research Box CM, Duke Station Durham, North Carolina	10
Chief of Ordnance Department of the Army Washington 25, D. C. Attn: ORDTB-PS	2
Deputy Chief of Staff for Logistics Department of the Army Washington 25, D. C. Attn: Research Br., R and	1
Commanding General Aberdeen Proving Ground, Maryland Attn: BRL	2
Commanding General Frankford Arsenal Bridesburg Station Philadelphia 37, Pennsylvania Attn: ORDBA-LC	2
Commanding General Picatinny Arsenal Dover, New Jersey Attn: S. Feltman, Ammo Lab	1
Commanding General Redstone Arsenal Huntsville, Alabama Attn: ORDDW-MR	1
Commanding General Rock Island Arsenal Rock Island, Illinois	1
Commanding Officer Springfield Armory Springfield 1, Massachusetts	1
Commanding Officer Watervliet Arsenal Watervliet, New York	1
Commanding Officer Watertown Arsenal Watertown 72, Massachusetts Attn: W. A. Laboratories	1
Commanding General Ordnance Weapons Command Rock Island, Illinois Attn: Research Branch	2
Chief, Detroit Ordnance District 574 E. Woodbridge Street Detroit 31, Michigan	2
Chief of Ordnance Department of the Army Washington 25, D. C. Attn: ORDGU-SE For transmittal to: Canadian Joint Staff 2001 Connecticut Ave., N.W. Washington 25, D. C.	1
Office of Naval Research Washington 25, D. C. Attn: Code 438	1
The Director Naval Research Laboratory Washington 25, D. C. Attn: Code 2021	1
Commanding Officer Office of Naval Research Branch Office Navy, 100, FPO New York, New York	2
Commander U. S. Naval Proving Ground Dahlgren, Virginia	1
U. S. Naval Ordnance Laboratory White Oak Silver Spring 19, Maryland Attn: Library Division	1

DISTRIBUTION LIST (Concluded)

Agency	Copy
Chief, Bureau of Ordnance (AD3) Department of the Navy Washington 25, D. C.	1
Director Air University Library Maxwell Air Force Base, Alabama	1
Commander Wright Air Development Center Wright-Patterson Air Force Base Ohio Attn: WCRRO	1
Commanding General Air Research and Development Command P. O. Box 1395 Baltimore 3, Maryland Attn: RDTOIL (Tech Library)	1
Commanding Officer Engineering Research and Development Laboratories Fort Belvoir, Virginia	1
Commanding Officer Frankford Arsenal Philadelphia 37, Pennsylvania Attn: S. Jarvis, Jr. Pittman-Dunn Labs.	
Armed Services Technical Information Agency Document Service Center Arlington Hall Station Arlington 12, Virginia	5
Director, Applied Physics Lab Johns Hopkins University 8621 Georgia Avenue Silver Spring 19, Maryland Attn: Dr. R. C. Herman	1
Technical Information Service P. O. Box 62 Oak Ridge, Tennessee Attn: Reference Branch	1
Director National Bureau of Standards Washington 25, D. C.	1
Professor S. I. Cheng Dept. of Aeronautical Engineering Princeton University Princeton, New Jersey	1